Wormholes in viscous cosmology

Deng Wang*
Theoretical Physics Division, Chern Institute of Mathematics, Nankai University, Tianjin 300071, China

Xin-He Meng†
Department of Physics, Nankai University, Tianjin 300071, China
State Key Lab of Theoretical Physics, Institute of Theoretical Physics, CAS, Beijing 100080, China

We study the wormhole spacetime configurations in bulk viscosity cosmology. Considering three classes of viscous models, i.e., bulk viscosity as a function of Hubble parameter H, temperature T and dark energy density ρ, respectively, we obtain nine wormhole solutions. Through the analysis for the anisotropic solutions, we conclude that, to some extent, these three classes of viscous models have very high degeneracy with each other. Subsequently, without the loss of generality, to investigate the traversabilities, energy conditions and stability for the wormhole solution, we study the wormhole solution of the constant redshift function of the viscous ωCDM model with a constant bulk viscosity coefficient. We obtain the following conclusions: the value of traversal velocity decreases for decreasing bulk viscosity, and the traversal velocity for a traveler depends on not only the wormhole geometry but also the effects of cosmological background evolution; the null energy condition will be violated more clearly when the bulk viscosity or the cosmic expansion velocity decreases; for the case of a positive surface energy density, the range of the junction radius decreases and the values of the parameter λ are further restricted when the throat radius of the wormhole r_0/M increases, bulk viscosity coefficient ζ_0 decreases and Hubble parameter H decreases, respectively; for the case of a negative surface energy density, by increasing r_0/M, decreasing ζ_0 and increasing H, the values of the parameter λ are less restricted, one may conclude that the total stability region increases, and the range of the junction radius increases, increases and decreases, respectively.

arXiv:1611.01614v1 [gr-qc] 5 Nov 2016

I. INTRODUCTION

In recent years, the cosmological observations has provided increasing evidence that our universe is under a phase of accelerated expansion [1, 2]. In order to explain the acceleration expansion phenomena, cosmologists during the past few decades introduce a new fluid, which possesses a negative enough pressure, named dark energy. According to the recent observational evidence, especially from the Type Ia supernovae project, the Sloan Digital Sky Survey (SDSS) project, the Wilkinson Microwave Anisotropy Probe (WMAP) satellite missions, the Planck satellite missions and galaxies clustering, we live in a favored spatially flat universe consisting approximately of 4% baryonic matter, 23% dark matter and 73% dark energy. The simplest candidate for dark energy is the cosmological constant scenario, Λ, first introduced by Einstein in order to keep the universe static, but dismissed soon when the universe is found to be undergoing an accelerated phase. So far, this mysterious constant has been reintroduced several times in history in attempts to explain several astrophysical phenomena, including most recently the flat spatial geometry implied by the Planck-2015 [3]. A cosmological constant is described by a single parameter, the inclusion of which brings the ΛCDM (Λ-Cold Dark Matter) model into excellent agreement with the current observations. However, there exist two fatal problems in this model [4]. The first one is the fine-tuning problem: theoretical estimates for the vacuum density are many orders of magnitude larger than its observed value, i.e., the famous 120-orders-of-magnitude discrepancy that makes the vacuum explanation suspicious. The second one is the coincidence problem, i.e., Ω_Λ and Ω_m are of the same order of magnitude only at present, which indicates our epoch as a very special time in the evolution of the universe. Besides, a positive cosmological constant is inconsistent with perturbed string theory [5]. Therefore, the actual origin of the dark energy might not be the Λ. This lack of a clear theoretical understanding has motivated the development of a wide variety of alternative models to describe the universe with dark energy.

In the present paper, we shall pay our attention to study the astrophysical scales properties in the universe by assuming the dark energy fluid is permeated everywhere rather than concentrating on studying the evolution of the universe. Moreover, in our entire universe, the existence of wormholes is a substantially appealing problem in physics both at micro and macro scales. There is no doubt that together with black holes, pulsars, quasars and white dwarfs,

*Electronic address: Cstar@mail.nankai.edu.cn
†Electronic address: xhm@nankai.edu.cn

etc., wormholes constituting the most intriguing and puzzling celestial bodies may provide a new window for new physics. Thus, it is very constructive necessary to make a brief review about the developments of wormholes.

A wormhole is a feature of space that is essentially a "shortcut" from one point in the universe to another point in the universe, allowing travel between them that is faster than it would take light to make the journey through the normal space. Thus, wormholes are tunnels or handles in the spacetime topology that connects different universes or widely separated regions of our universe via a throat. The earliest significant contribution we are aware of is the introduction, in 1935, of the object now referred to as Einstein-Rosen bridge [6]. This field then lay dormant for twenty years until Wheeler first coined the term " wormhole " and introduced his idea of" spacetime foam " [3]. A thirty year interregnum followed, punctuated by isolated contributions, until the major revival of interest following the 1988 paper by Morris and Thorne [8]. In their elegant work, a new class of solutions of the Einstein field equations was presented, which describe wormholes that, in principle, could be traversable by human beings. It is essential in these solutions that the wormhole possesses a throat at which there is no horizon. In the meanwhile, this property, together with the field equations, places an extreme constraint on the material that generates the wormhole spacetime curvature. This leads to such material must violate all the energy conditions (null, weak, strong and dominant) that underlie some deeply cherished theorems in general relativity. Nonetheless, we could not easily rule out the existence of the material; and quantum field theory gives tantalizing hints that such material might, in fact, be possible. More specifically, they prove black holes are unstable for interstellar travel and Schwarzschild wormholes is non-traversable, analyze the properties of traversable wormholes, calculate out the mathematical details of traversable wormholes and explore the stability of the wormhole. Subsequently, Visser [9] and Possion and Visser [10] conjectured that all " exotic " matter is confined to a thin shell between universes. Their model is constructed surgically by grafting two Schwarzschild spacetimes together so that no horizon exists. It is so-called thin shell wormholes which has been widely investigated by many authors in various alternative cosmological models and theories of gravity. Furthermore, Visser et al. develops the notion of " volume integral quantifier " (VIQ), and one may obtain the total amount of energy condition violating matter by calculating the VIQ [11]. After that, the subject has grown substantially, and it is now almost out of control and there are many branches out of the special space-time structures etc., such as energy conditions, theoretical construction, stability, time machines, and astrophysical signatures. A quarter century later, a follow-up is written by Thorne which has two purposes [12]:

⋆ to explain how Interstellar's wormhole images were constructed and explain the decisions made on the way to their final form.

⋆ to present this explanation that may be useful to students and teachers in elementary courses on general relativity.

We could find that the follow-up emphasize mainly the feasibility and the real status of wormholes in our real universe.

Recently, because of the new discovery that our universe is undergoing an accelerated expansion, an increasing interest to the subjects has arisen significantly in connection with the discovery. Since in both cases the null energy condition (NEC), $T_{\mu\nu}k^{\mu}k^{\nu} > 0$, is violated and consequently all of other energy conditions, where $T_{\mu\nu}$ is the stress-energy tensor and k^{μ} any future directed null vector. Therefore, an interesting and surprising overlap between two seemingly separated subjects occurs. A simple way to parameterize the dark energy is by an equation of state of this form $-K = p/\rho$, where p is the spatially homogeneous pressure and ρ the energy density of the dark energy. A value of $K > 1/3$ is required for cosmic expansion, and $K = 1$ a cosmological constant. The particular case $K = 2/3$ is extensively analyzed in [13]. In quintessence models, the parameter range is $1/3 < K < 1$ and the dark energy decreases with a scale factor $a(t)$ as $\rho \propto a^{3(K-1)}$. In phantom models, the the parameter range is $K > 1$ and we can also find that the NEC is naturally violated, $p + \rho < 0$, in the phantom case.

In the literature, all the authors almost construct wormholes by only using the linear equation of state, namely, assuming that the universe is filled with a perfect fluid. However, the dynamical behaviors of the true universe are physically dominated by a non-ideal cosmological fluid. Based this concern, in our previous works [14, 15], we have investigated the wormhole spacetime configurations in a non-ideal fluid universe by using the Shan-Chen equation of state. Actually, it is worth noting that the the Shan-Chen cosmology is essentially equivalent to the viscous cosmology. In the present paper, we are dedicated to investigate the wormholes in the bulk viscous cosmology. Two authors have studied some aspects of wormholes in the bulk viscosity cosmology: Hristu Culetu develops a classical membrane model for a dynamical wormhole [16]. This model leads to an expanding throat and a negative bulk viscosity coefficient $-1/6\pi$ on the throat, implying the instability against perturbations; Mubasher Jamil has investigated the effects of the accretion of phantom energy with non-zero bulk viscosity onto a Morris-Thorne wormhole, and find that if the bulk viscosity is enough large, the mass of wormhole increases rapidly as compared to small or zero bulk viscosity [17]. Furthermore, we are aiming at obtaining the clear expressions of the shape function and the redshift function in the solutions of Einstein field equations, and study the related properties and characteristics of the obtained wormhole spacetime structure. More precisely, we explore the wormhole configurations in different viscous models starting from the bulk viscosity equation of state. From this, we should review the history of bulk viscosity and its applications in modern cosmology and theories of gravity.

We have felt an increasing interest and attention in viscous cosmology during the past several decades. This contrasts the traditional approach, in which the cosmic fluid has usually be taken to be perfect (non-viscous). From a hydrogynamicist's point of view this is to some extent surprising, since there are several situations in fluid mechanics, even in homogeneous space without boundaries, where the inclusion of viscosity becomes mandatory. Especially, this is so in connection with turbulence phenomena. In history, perfect fluid models have for a long time been used in cosmological theory and the introduction of viscosity concepts came later. Misner was probably the first to introduce viscosity in cosmological theory in connection with his study of how initial anisotropies in the early universe become relaxed [18]. Grøn has given an extensive review of the subject, the reader is referred to it for detailed information [19]. Recently, Dou and Meng, Ma and Meng, Nojiri and Brevik give new different reviews from different points of view, the reader is referred to them for more details [20–23].

As is well known, the perfect fluid assumption is assertive since it implies no dissipation, which actually exists widely and intuitively play a crucial role in the evolution of the universe, especially in the very early hot stages. To be more realistic, models of imperfect fluid are invoked by introducing viscosity into investigation. More precisely, to the first order in deviation from thermal equilibrium there are two such coefficients, the shear viscosity ξ, most often being the dominant one, and the bulk viscosity ζ [24]. The simplest theory of this kind is the case of a constant bulk viscosity, regarded as a equivalence to the cosmological constant scenario. A widely investigated case is that bulk viscosity as a function of Hubble parameter, which has been proved to be well consistent with observed late-time acceleration and recover both the matter and dark energy dominant eras. Another intriguing case is that bulk viscosity behaves as a parameterized power-law with respect to the matter density, which could be shown to be similar to the Chaplygin gas model. In addition, temperature-dependent viscosity from classical statistical physics is introduced into observational cosmology and behaves well as compared with the observed data. Furthermore, viscosity term containing high derivatives of scale factor and redshift is also considered as a more general theory [25–30]. In the past few years, viscosity-induced crossing of the phantom barrier in Einstein gravity and modified gravity and various models of dark energy coupled with dark matter in a dissipative universe is studied. Especially in some special cases, the Little Rip, Pseudo Rip and bounce cosmological models can be related to each other via the bulk viscosity concept. Moreover, it is necessary to note that viscous Ricci dark energy (RDE) is also considered in the literature [31]. In the RDE model without bulk viscosity, the universe is younger than some old objects at some redshifts. Since the age of the universe should be longer than any objects in the universe, the RDE model suffers the age problem, especially when we consider the object APM $08279+5255$ at $z=3.91$, whose age is $t=2.1$ Gyr, z being the redshift. Nevertheless, once the bulk viscosity effect is taken into account, this age problem is alleviated. In this paper, we focus on the aspects of wormhole physics of three classes of models in the bulk viscous cosmology: bulk viscosity as a function of Hubble parameter, temperature and matter density, respectively. In what follows, it is necessary to make a brief review for the basic formalism of the viscous cosmology.

We use the convention in which the Minkowski metric is $(-1,1,1,1)$. Greek indices are summed from 0 to 3, Latin indices are summed from 1 to 3. In the scheme of imperfect fluids, the energy stress tensor can be written as in the following manner,

$$T_{\mu\nu}=\rho U_\mu U_\nu+(p-\theta\zeta)h_{\mu\nu}-2\xi\sigma_{\mu\nu}+Q_\mu U_\nu+Q_\nu U_\mu, \tag{1}$$

where ρ is the mass-energy density, p the isotropic pressure, $U_\mu=(1,0,0,0)$ the four-velocity of the cosmic fluid in comoving coordinates, $h_{\mu\nu}=g_{\mu\nu}+U_\mu U_\nu$ the projection tensor, $\omega_{\mu\nu}=h^\iota_\mu h^\upsilon_\nu U_{[\iota;\upsilon]}=\frac{1}{2}(U_{\mu;\iota}h^\iota_\nu-U_{\nu;\iota}h^\iota_\mu)$ the rotation tensor, $\theta_{\mu\nu}=h^\iota_\mu h^\upsilon_\nu U_{(\iota;\upsilon)}=\frac{1}{2}(U_{\mu;\iota}h^\iota_\nu+U_{\nu;\iota}h^\iota_\mu)$ is the expansion tensor, $\theta=\theta^\nu_\mu=U^\mu_{;\mu}$ the expansion scalar, $\sigma_{\mu\nu}=\theta^\nu_\mu-\frac{1}{3}h^\nu_\mu\theta$, ζ the bulk viscosity, ξ the shear viscosity, $U_{\mu;\nu}=\omega_{\mu\nu}+\sigma_{\mu\nu}+\frac{1}{3}h^\nu_\mu\theta-A_\mu U_\nu$ the decomposition of the covariant derivative of the fluid velocity, $A_\nu=\dot{U}_\mu=U_\nu U_{\mu;\nu}$ the four-acceleration of the fluid, and $Q^\mu=-\kappa h^{\mu\nu}(T_{,\nu}+TA_\nu)$ the heat flux density four-vector with k the thermal conductivity.

In the case of thermal equilibrium, $Q_\mu=0$, additionally, the term of shear viscosity vanished when a completely isotropic universe is assumed. In the isotropic and homogeneous Friedmann-Robertson-Walker (FRW) metric, Eq.(1) can be rewritten as

$$T_{\mu\nu}=\rho U_\mu U_\nu+(p-\theta\zeta)h_{\mu\nu}, \tag{2}$$

where $\theta=3H=3\frac{\dot{a}}{a}$ and the dot denotes differential with respect to the cosmic time t.

In general, wormholes can be classified into two categories-Euclidean wormholes and Lorentzian wormholes based on the famous Gorech theorem. The Euclidean wormholes comes from Euclidean quantum gravity and the Lorentzian wormholes that are static spherically symmetric solutions of Einstein field equations. Here we just explore the Lorentzian wormholes in a viscous universe. It is worth noting that our work is mainly motivated by three earlier studies [32–34] that have demonstrated the possible existence of wormholes in the outer regions of the galactic halo and in the central parts of the halo, respectively, based on NFW (Navarro-Frenk-White) density profile and the URC (Universal Rotation Curve) dark matter model [35]. Especially, the second result is an important compliment to

the earlier result, thereby confirming the possible existence of wormholes in most of the spiral galaxies. After their interesting and suggestive works, immediately, A. Övgün et al. considered the existence of wormholes in the spherical stellar systems. In addition, it is shown that based on the Einasto model [36–38] wormholes in the outer regions of spiral galaxies are possible while the central regions prohibit such space-time structure formations.

The rest of this paper is outlined in the following manner. In the next section, we make a review of mathematical details about wormhole calculations and assume the simplest anisotropic pressure for cosmic fluid. In Section 3, there are three classes of viscous models to be discussed and obtain nine solutions in which, for every model, we solve the Einstein equations by both inserting the shape function $b(r) = r_0 + \frac{1}{K}(r - r_0)$ and the redshift function $\Phi = C$: in Subsection 1, we investigate the wormhole solutions where the bulk viscosity as a function of Hubble parameter H, and consider the relatively simple linear model, not involving the quadratic term H^2, and power law model; in Subsection 2, we consider the bulk viscosity as a function of temperature T and analyze the power law model and obtain two solutions; in Subsection 3, we study the viscosity term as a function of the dark energy density ρ, similarly, explore the power law model and obtain two solutions. In Sections $4-6$, as a concrete case, we investigate the traversabilities, energy conditions and stability for the wormhole solution of the constant redshift function of the viscous ωCDM model with a constant bulk viscosity coefficient. In the final section, we discuss and conclude (we use units $G = c = 1$).

II. WORMHOLES AS SPECIAL SPACE-TIME STRUCTURES

In the present study, we consider a spacetime metric for the wormholes in a static spherically symmetric form

$$ds^2 = -Udt^2 + \frac{dr^2}{V} + r^2 d\Omega^2, \tag{3}$$

and U and V can be defined as

$$V = 1 - \frac{b(r)}{r}, \quad U = e^{2\Phi(r)}, \tag{4}$$

where r is the radial coordinate which runs in the range $r_0 \leq r < \infty$ (r_0 is the throat radius of the wormhole), and $d\Omega^2$ is the unit line element on the sphere. To form a wormhole, the redshift function $\Phi(r)$ should be finite and non-vanishing in order to avoid an event horizon in the vicinity of r_0, and the shape function $b(r)$, which determines the spatial shape of the wormhole when viewed, must obey the usual flare-out conditions at the throat

$$b(r_0) = r_0, \tag{5}$$

$$b'(r_0) < 1, \tag{6}$$

$$b(r) < r, r > r_0. \tag{7}$$

If one expects to obtain a traversable wormhole, the asymptotically flatness condition is required, that is, $b(r)/r \to 0$ as $r \to \infty$. Utilizing the Einstein field equation, $G_{\alpha\beta} = 8\pi T_{\alpha\beta}$, in an orthonormal reference frame, we have the following equations

$$\frac{b'}{8\pi r^2} = \rho(r), \tag{8}$$

$$\frac{U'}{U} = \frac{8\pi p_r r^3 + b}{r(r-b)}, \tag{9}$$

where $T^t_t = -\rho, T^r_r = p_r, T^\mu_\nu$ is the stress-energy tensor.

One can also derive from the conservation law of the stress-energy tensor $T^\nu_{\mu;\nu} = 0$ with $\mu = r$, which can be interpreted as the hydrostatic equation for equilibrium for the material threading the wormhole, that

$$p_\perp = \frac{r}{2}[p'_r + \frac{2p_r}{r} + \frac{U'}{2U}(p_r + \rho)], \tag{10}$$

where $T^\theta_\theta = T^\phi_\phi = p_\perp$. In addition, we assume the pressures are anisotropic and just consider the simplest case between the tangential pressure and the energy density but with $p_\perp \neq p_r$,

$$p_\perp = \alpha\rho. \tag{11}$$

III. MODELS

A. bulk viscosity as a function of Hubble parameter: $\zeta = \zeta(H)$

1. *linear model:* $\zeta = \zeta_0 + \zeta_1 H$

For the linear models, we just consider the relatively simple case, where the bulk viscosity can be expressed as

$$\zeta = \zeta_0 + \zeta_1 H, \tag{12}$$

where ζ_0 and ζ_1 are two constants conventionally. Hence, the radial pressure is

$$p_r = -K\rho - 3\zeta_0 H - 3\zeta_1 H^2. \tag{13}$$

It is easy to see that the bulk viscosity coefficient reduces to be a constant when $\zeta_1 = 0$. Here we consider two specific shape functions that are widely investigated in the literature. At first, we take the shape function $b(r) = r_0 + \frac{1}{K}(r - r_0)$, then Eqs. (8-9) become

$$\rho(r) = \frac{1}{8K\pi r^2}, \tag{14}$$

$$\frac{U'}{U} = -\frac{1}{r} - \frac{24\pi H(\zeta_0 + \zeta_1 H)r^2}{(r - r_0)(1 - \frac{1}{K})}, \tag{15}$$

it follows that

$$U(r) = \frac{A}{r} e^{\frac{12HK\pi(\zeta_0+\zeta_1 H)[r(2r_0+r)+2r_0^2\ln(r-r_0)]}{1-K}}. \tag{16}$$

Thus, the metric becomes

$$ds^2 = -\frac{A}{r} e^{\frac{12HK\pi(\zeta_0+\zeta_1 H)[r(2r_0+r)+2r_0^2\ln(r-r_0)]}{1-K}} dt^2 + \frac{dr^2}{(1 - \frac{1}{K})(r - r_0)} + r^2 d\Omega^2, \tag{17}$$

where A is an arbitrary constant that affects the normalization of time.

Then the next step is to calculate out the α in Eq. (11). Substitute Eq. (11) and Eq. (13) and Eqs. (14-15) into Eq. (10), we can obtain

$$\alpha = \alpha(r) = \frac{K-1}{4} - 18\pi KHr^2(\zeta_0 + \zeta_1 H) + \frac{6\pi KHr^3(\zeta_0 + \zeta_1 H)}{r - r_0} + \frac{144\pi^2 K^2 H^2 r^5(\zeta_0 + \zeta_1 H)^2}{(r - r_0)(K - 1)}. \tag{18}$$

One can find that α is a function of the radial coordinate r, which is similar to our previous work but different from Zaslavskii's work [39], since we consider the non-ideal equation of state here.

The second possibility is $b(r) = \sqrt{r_0 r}$, obviously, which also satisfies the flare-out conditions. By using the same step as the first one, we get

$$\frac{U'}{U} = \frac{(1 - \frac{K}{2})(r_0 r)^{\frac{1}{2}} - 24\pi H(\zeta_0 + \zeta_1 H)r^3}{r[r - (r_0 r)^{\frac{1}{2}}]}. \tag{19}$$

Solving this equation, we obtain

$$U(r) = e^{\frac{1}{2}\{(K-2)\ln(r) - 48H\pi(\zeta_0+\zeta_1 H)(r+2\sqrt{r_0 r}) + [K-2+48r_0 H\pi(\zeta_0+\zeta_1 H)][2\arctan(\sqrt{\frac{r}{r_0}}) - \ln(r-r_0)]\}}. \tag{20}$$

Hence, the solution is

$$ds^2 = -e^{\frac{1}{2}\{(K-2)\ln(r) - 48H\pi(\zeta_0+\zeta_1 H)(r+2\sqrt{r_0 r}) + [K-2+48r_0 H\pi(\zeta_0+\zeta_1 H)][2\arctan(\sqrt{\frac{r}{r_0}}) - \ln(r-r_0)]\}} dt^2 + \frac{dr^2}{(1 - \sqrt{\frac{r_0}{r}})} + r^2 d\Omega^2. \tag{21}$$

Based on our previous work, we can also insert the redshift function $\Phi = C$ into Eq. (9) by hand

$$\frac{Kb'}{r^2} - b + 24\pi H(\zeta_0 + \zeta_1 H)r^3 = 0, \tag{22}$$

it follows that

$$b(r) = C_1 e^{\frac{r^3}{3K}} + 24H\pi(3K + r^3)(\zeta_0 + \zeta_1 H), \tag{23}$$

where C_1 can be obtained through using the condition $b(r_0) = r_0$

$$C_1 = [r_0 - 24H\pi(3K + r_0^3)(\zeta_0 + \zeta_1 H)]e^{-\frac{r_0^3}{3K}}. \tag{24}$$

So we can get

$$b(r) = e^{\frac{r^3 - r_0^3}{3K}}[r_0 - 24H\pi(3K + r_0^3)(\zeta_0 + \zeta_1 H)] + 24H\pi(3K + r^3)(\zeta_0 + \zeta_1 H), \tag{25}$$

and the solution becomes

$$ds^2 = -e^{2C}dt^2 + \frac{dr^2}{1 - \frac{e^{\frac{r^3 - r_0^3}{3K}}[r_0 - 24H\pi(3k + r_0^3)(\zeta_0 + \zeta_1 H)] + 24H\pi(3K + r^3)(\zeta_0 + \zeta_1 H)}{r}} + r^2 d\Omega^2. \tag{26}$$

2. power law model: $\zeta = \eta H^\delta$

In this model, the radial pressure that contains the bulk viscosity term can be expressed as follows

$$p_r = -K\rho - 3\eta H^{1+\delta}. \tag{27}$$

and we just consider two cases $b(r) = r_0 + \frac{1}{K}(r - r_0)$ and $\Phi = C$. For the first case, we can obtain

$$U(r) = \frac{C}{r} e^{-12K\pi\eta H^{1+\delta}}[r(2r_0 + r) + 2r_0^2 ln(r - r_0)]. \tag{28}$$

Hence, the metric is

$$ds^2 = -\frac{C}{r} e^{-12K\pi\eta H^{1+\delta}}[r(2r_0 + r) + 2r_0^2 ln(r - r_0)]dt^2 + \frac{dr^2}{(1 - \frac{1}{K})(r - r_0)} + r^2 d\Omega^2, \tag{29}$$

at the same time, we still suppose the anisotropic pressure is $p_\perp = \alpha\rho$, it follows that

$$\alpha(r) = \frac{K - 1}{4} - 18\pi K\eta H^{1+\delta} r^2 + \frac{6\pi K\eta H^{1+\delta} r^3}{r - r_0} + \frac{144\pi^2\eta^2 K^2 H^{2(1+\delta)} r^5}{(r - r_0)(K - 1)}. \tag{30}$$

For the second case, inserting $\Phi = C$ and Eq. (13) into Eq. (9) by hand, we get

$$\frac{Kb'}{r^2} - b + 24\pi\eta H^{1+\delta} r^3 = 0, \tag{31}$$

it follows that

$$b(r) = C_1 e^{\frac{r^3}{3K}} + 24\pi\eta H^{1+\delta}(3K + r^3), \tag{32}$$

$$C_1 = [r_0 - 24\pi\eta H^{1+\delta}(3K + r_0^3)]e^{-\frac{r_0^3}{3K}}. \tag{33}$$

Substituting Eq. (33) into Eq. (32), we can obtain

$$b(r) = e^{\frac{r^3 - r_0^3}{3K}}[r_0 - 24\pi\eta H^{1+\delta}(3K + r_0^3)] + 24\pi\eta H^{1+\delta}(3K + r^3), \tag{34}$$

so the solution is

$$ds^2 = -e^{2C}dt^2 + \frac{dr^2}{1 - \frac{e^{\frac{r^3 - r_0^3}{3K}}[r_0 - 24\pi\eta H^{1+\delta}(3K + r_0^3)] + 24\pi\eta H^{1+\delta}(3K + r^3)}{r}} + r^2 d\Omega^2. \tag{35}$$

B. bulk viscosity as a function of temperature: $\zeta = \zeta(T)$

In this model, we consider the bulk viscosity as

$$\zeta = \xi T^{\epsilon}, \tag{36}$$

so the radial pressure of our new fluid model can be written as

$$p_r = -K\rho - 3H\xi T^{\epsilon}. \tag{37}$$

For this model, similarly, we investigate the first case through inserting the shape function $b(r) = r_0 + \frac{1}{K}(r - r_0)$ into Eq. (9) by hand, we can get

$$\frac{U'}{U} = -\frac{1}{r} - \frac{24\pi\xi H T^{\epsilon} r^2}{(r - r_0)(1 - \frac{1}{K})}, \tag{38}$$

it follows that

$$U(r) = \frac{C}{r} e^{-12K\pi\xi H T^{\epsilon}} [r(2r_0 + r) + 2r_0^2 ln(r - r_0)]. \tag{39}$$

Therefore, we can get the metric

$$ds^2 = -\frac{C}{r} e^{-12K\pi\xi H T^{\epsilon}} [r(2r_0 + r) + 2r_0^2 ln(r - r_0)]dt^2 + \frac{dr^2}{(1 - \frac{1}{K})(r - r_0)} + r^2 d\Omega^2. \tag{40}$$

Then we continue considering the simplest anisotropic pressure $p_{\perp} = \alpha\rho$. After substituting Eq. (11), Eq. (14) and Eqs. (37-38) into Eq. (10), we have

$$\alpha(r) = \frac{K - 1}{4} - 18K\pi\xi H T^{\epsilon} r^2 + \frac{6K\pi\xi H T^{\epsilon} r^3}{r - r_0} + \frac{144\pi^2\xi^2 K^2 H^2 T^{2\epsilon} r^5}{(r - r_0)(K - 1)}. \tag{41}$$

Another case is still $\Phi = C$, we can easily get

$$b(r) = C_1 e^{\frac{r^3}{3K}} + 24H\xi\pi T^{\epsilon}(3K + r^3), \tag{42}$$

$$C_1 = [r_0 - 24H\xi\pi T^{\epsilon}(3K + r_0^3)] e^{-\frac{r_0^3}{3K}}. \tag{43}$$

Thus, it follows that

$$b(r) = e^{\frac{r^3 - r_0^3}{3K}} [r_0 - 24H\xi\pi T^{\epsilon}(3K + r_0^3)] + 24H\xi\pi T^{\epsilon}(3K + r^3), \tag{44}$$

so the solution is

$$ds^2 = -e^{2C} dt^2 + \frac{dr^2}{1 - \frac{e^{\frac{r^3 - r_0^3}{3K}} [r_0 - 24H\xi\pi T^{\epsilon}(3K + r_0^3)] + 24H\xi\pi T^{\epsilon}(3K + r^3)}{r}} + r^2 d\Omega^2. \tag{45}$$

C. bulk viscosity as a function of energy density: $\zeta = \zeta(\rho)$

In this situation, we just consider the power law model, i.e., the bulk viscosity coefficient can be expressed as

$$\zeta = \beta\rho^{\gamma}, \tag{46}$$

where β and γ are arbitrary constants, $\beta > 0$ ensures a positive entropy at the request of the second law of thermaldynamics. So the radial pressure after substituting Eq. (11) into Eq. (44) becomes

$$p_r = -\frac{1}{8\pi r^2} - 3H\beta(8\pi K r^2)^{-\gamma}. \tag{47}$$

In the first place, we still start from the shape function $b(r) = r_0 + \frac{1}{K}(r - r_0)$, then Eq. (9) is

$$\frac{U'}{U} = -\frac{1}{r} - \frac{24\pi\beta H\rho^{\gamma}r^2}{(r - r_0)(1 - \frac{1}{K})}, \tag{48}$$

we obtain by using Eq. (47) in Eq. (48)

$$U(r) = \frac{C}{r}e^{-12K\pi\beta H\rho^{\gamma}}[r(2r_0 + r) + 2r_0^2 ln(r - r_0)]. \tag{49}$$

Hence, the metric is

$$ds^2 = -\frac{C}{r}e^{-12K\pi\beta H\rho^{\gamma}}[r(2r_0 + r) + 2r_0^2 ln(r - r_0)]dt^2 + \frac{dr^2}{(1 - \frac{1}{K})(r - r_0)} + r^2 d\Omega^2. \tag{50}$$

It is worth noting that the energy density ρ still represents $\frac{1}{8K\pi r^2}$. Similarly, here we just consider the anisotropic pressure as $p_{\perp} = \alpha\rho$ and we have through some calculations

$$\alpha(r) = \frac{K - 1}{4} - \frac{3}{2}\gamma\beta H(8\pi K)^{2-\gamma}r^{5-2\gamma} - \frac{9}{4}H\beta(8\pi K r^2)^{1-\gamma} + \frac{6\pi K\beta\rho^{\gamma}r^3}{r - r_0} + \frac{18K\beta^2H^2\rho^{\gamma}(8\pi K)^{1-\gamma}r^{5-2\gamma}}{(r - r_0)(K - 1)}. \tag{51}$$

In the second place, through assuming the redshift function $\Phi = C$ and inserting it and Eq. (8) into Eq. (9) we can have

$$\frac{Kb'}{r^2} - b + 24\pi H\beta(\frac{b'}{8\pi r^2})^{\gamma}r^3 = 0. \tag{52}$$

Here we just concentrate on the case of γ=1, then Eq. (50) can be analytically solved as follows

$$b(r) = C_1(K + 3Hr^3\beta)^{\frac{1}{9H\beta}}. \tag{53}$$

Use the condition $b(r_0) = r_0$ once again,

$$C_1 = r_0(K + 3Hr_0^3\beta)^{-\frac{1}{9H\beta}}, \tag{54}$$

After substitution of Eq. (54) into Eq. (53), we get

$$b(r) = r_0(\frac{K + 3Hr^3\beta}{K + 3Hr_0^3\beta})^{\frac{1}{9H\beta}}. \tag{55}$$

So the metric is

$$ds^2 = -e^{2C}dt^2 + \frac{dr^2}{1 - \frac{r_0}{r}(\frac{K+3Hr^3\beta}{K+3Hr_0^3\beta})^{\frac{1}{9H\beta}}} + r^2 d\Omega^2. \tag{56}$$

It is worth noting that the anisotropic solutions for the case $b(r) = r_0 + \frac{1}{K}(r - r_0)$ in three different physical considerations from Eq. (18), Eq. (30), Eq. (41) and Eq. (51) have substantial high degeneracy with each other. To be more precise, the first term $\frac{K-1}{4}$ in these equations corresponds to the anisotropic solution of the ideal cosmic fluid. In principle, one can obtain the same expression of anisotropic solution by choosing appropriately the parameters ζ_0, ζ_1, H, η, δ, ξ, ϵ, T, γ, β and ρ. Thus, to some extent, these three viscous models have very high degeneracy with each other.

IV. TRAVERSABILITIES ANALYSIS

To perform the traversabilities analysis, we consider the case of the constant redshift function for the linear model $\zeta = \zeta_0 + \zeta_1 H$, therefore, the corresponding shape function is shown in Eq. (25). Without the loss of generality, we set $\zeta_1 = 0$, thus, the shape function can be rewritten as

$$b(r) = e^{\frac{r^3 - r_0^3}{3K}}[r_0 - 24H\pi\zeta_0(3K + r_0^3)] + 24H\pi\zeta_0(3K + r^3), \tag{57}$$

It is easy to be seen that this solution is only traversable but not asymptotically flat, since Φ is finite and $b/r \to 0$ when $r \to \infty$. Hence, the dimensions of this wormhole may be very finite.

As noted in our previous works [40, 41], three conditions must be satisfied for a human being in the spaceship who intends to journey through the wormhole: (i) The acceleration felt by the travelers should not exceed 1 Earth's gravitational acceleration g; (ii) The tidal acceleration should not exceed 1 Earth's gravitational acceleration g; (iii) The traverse time measured by the travelers and the observers who keep at rest at the space station should satisfy the several quantitative relationships. More mathematical details can be found in [42].

For the conveniences of calculations, we obtain the key formula through some simple derivations as follows

$$v \leq r_0 \sqrt{\frac{Kg}{r_0^3 - 24H\pi\zeta_0 r_0^5 - K}}, \tag{58}$$

Subsequently, assuming the throat radius of the wormhole $r_0 = 10$ m, the dark energy equation of state parameter $K = 2$, the recent Hubble parameter $H = 73.24\ kms^{-1}Mpc^{-1}$ and the bulk viscosity coefficient $\zeta_0 = 10^{-6}$, we obtain the traversal velocity $v \approx 2.10$ m/s. Furthermore, we find that the value of traversal velocity decreases for decreasing bulk viscosity, and approaches $v \approx 1.40$ m/s. In the meanwhile, we also find that the traversal velocity for a traveler depends on not only the wormhole geometry (r_0) but also the effects of cosmological background evolution (K, ζ_0 and H). Note that, in the above, we actually compute out the traversal velocity of the viscous ωCDM model with a constant bulk viscosity coefficient.

V. ENERGY CONDITIONS

Generally speaking, there are two important kinds of energy condition in classical general relativity, namely, the point-wise energy conditions and averaged energy conditions. The point-wise energy conditions usually include the above-mentioned NEC, the weak energy condition (WEC), the strong energy condition (SEC) and the dominant energy condition (DEC). More precisely, the corresponding mathematical descriptions for different energy conditions in a spatially flat Friedmann-Robertson-Walker (FRW) universe are expressed as

$\star$ NEC $\Leftrightarrow \rho + p \geqslant 0$,
$\star$ WEC $\Leftrightarrow \rho + p \geqslant 0$ and $\rho \geqslant 0$,
$\star$ SEC $\Leftrightarrow \rho + p \geqslant 0$ and $\rho + 3p \geqslant 0$,
$\star$ DEC $\Leftrightarrow \rho \pm p \geqslant 0$ and $\rho \geqslant 0$.

It is worth noting that, mathematically, the NEC is the necessary condition of the other three energy conditions. In what follows, we would like to investigate the behaviors of different energy conditions in astrophysical scales and explore the effects of the bulk viscosity on the energy conditions. Here we still consider the above-mentioned case $\Phi = C$ and $p = -K\rho - 3\zeta_0 H$. Subsequently, using Eq. (8) and Eq. (57), one can easily obtain the NEC as

$$p + \rho = \frac{1-K}{8\pi}\{\frac{e^{\frac{r^3 - r_0^3}{3K}}}{K}[r_0 - 24H\pi\zeta_0(3K + r_0^3)] + 72H\pi\zeta_0\} - 3\zeta_0 H \geqslant 0. \tag{59}$$

Furthermore, in the left panel of Fig. 1, we find that the NEC will be violated more clearly when the bulk viscosity decreases, for given throat radius of the wormhole r_0, dark energy equation of state parameter K and Hubble parameter H. In the medium panel of Fig. 1, using the recent Planck's result and A. Riess et al.'s result [3, 43], we also show that the NEC is violated more clearly when the value of the Hubble parameter decreases, for given bulk viscosity coefficient ζ_0, throat radius of the wormhole r_0 and dark energy equation of state parameter K. This means that, the more clearly the NEC is violated, the smaller the cosmic expansion velocity is. In the right panel of Fig. 1, we also exhibit the relations between different energy conditions and the radial coordinate r, and find that the NEC, DEC and SEC are always violated when $r > r_0$, except for $\rho \geqslant 0$ of the WEC is satisfied all the time for given parameters ζ_0, K, r_0 and H. Physically, the non-violation of the WEC indicates that the dark energy fluid in the viscous ωCDM model has a non-diverging effect on congruences of null geodesics. However, since the NEC in this case is violated, all the point-wise energy conditions are always violated when $r > r_0$.

VI. STABILITY ANALYSIS

In this section, we are aiming at investigating the effects of the bulk viscosity on stability of the wormhole spacetime configuration. Concretely, we still take into account the case of $\Phi = C$ and $p = -K\rho - 3\zeta_0 H$. Furthermore, we conclude the method in [42] as follows:

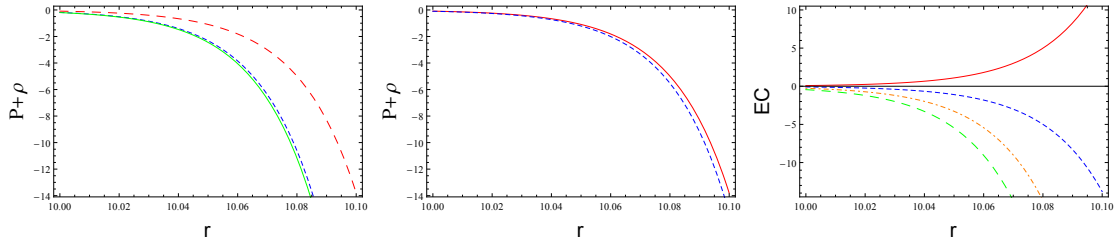

FIG. 1: The left panel represents the relation between $p+\rho$ and r: for given throat radius of the wormhole $r_0 = 10$ m, dark energy equation of state parameter $K = 2$ and Hubble parameter $H = 73.24\ kms^{-1}Mpc^{-1}$, the red (long-dashed) line corresponds to the case $\zeta_0 = 10^{-6}$, the blue (short-dashed) line $\zeta_0 = 10^{-7}$ and the green (solid) line $\zeta_0 = 10^{-8}$. The medium panel represents the relation between $p+\rho$ and r: for given throat radius of the wormhole $r_0 = 10$ m, dark energy equation of state parameter $K = 2$ and the bulk viscosity coefficient $\zeta_0 = 10^{-6}$, the red (solid) line corresponds to $H = 73.24\ kms^{-1}Mpc^{-1}$ and the blue (dashed) line $H = 66.93\ kms^{-1}Mpc^{-1}$ (note that we just take the best fitting value of the Hubble parameter). The right panel represents the relations between different energy conditions and r: for given parameters $\zeta_0 = 10^{-6}$, $K = 2$, $r_0 = 10$ m and $H = 73.24\ kms^{-1}Mpc^{-1}$, the red (solid) line corresponds to ρ, the blue (short-dashed) line $p+3\rho$, the orange line $p+\rho$, the green (long-dashed) line $p-\rho$ and the horizontal line zero.

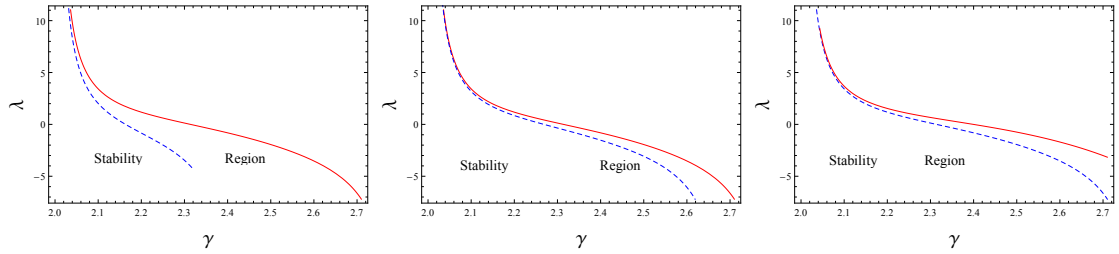

FIG. 2: Plots for a positive surface energy density, i.e., $b(a_0) < 2M$. In the left panel, we set the parameters $K = 2$, $H = 73.24$ and $\zeta_0 = 10^{-6}$ for both cases. The red (solid) and blue (dashed) lines represent $r_0/M = 0.1$ and $r_0/M = 0.25$, respectively. In the medium panel, we set the parameters $K = 2$, $H = 73.24$ and $r_0/M = 0.1$ for both cases. The red (solid) and blue (dashed) lines represent $\zeta_0 = 10^{-6}$ and $\zeta_0 = 10^{-10}$, respectively. In the right panel, we set the parameters $K = 2$, $r_0/M = 0.1$ and $\zeta_0 = 10^{-6}$ for both cases. The red (solid) and blue (dashed) lines represent $H = 150$ and $H = 73.24$, respectively. The stability regions are shown beneath these curves.

⋆ Use the Darmois-Israel formalism to derive the so-called Lanczos equation, and match an exterior Schwarzschild geometry into the interior traversable wormhole geometry.

⋆ Work out the nontrivial components of the extrinsic curvature, the surface energy density σ and tangential pressure P, the defined physical quantity Ξ and the radial derivative of the surface energy density σ'. Note that these quantities are all the functions of the junction radius a.

⋆ Utilize the equation of motion and linearize around a stable solution situated at a_0 to derive the equilibrium relation and the stability condition.

⋆ Define a new quantity λ to characterize the stable equilibrium and combine the master equation and the aforementioned stability condition to reexpress the stability condition (see Eqs. (41-42) in [42]). Note that the new stable condition shall be discussed separately in the cases of a positive and a negative surface energy density.

⋆ Substitute the redshift function $\Phi(a)$ and the shape function $b(a)$ of a given cosmological scenario into the new stable condition, so that one can get the final stability expression. However, in general, these results shall be exhibited graphically since the expression of the parameter λ is substantially cumbersome.

In what follows, we would like to discuss separately the cases of $b(a_0) < 2M$ and $b(a_0) > 2M$, i.e., the cases of a positive and a negative surface energy density.

For the case of $b(a_0) < 2M$, we obtain the range of the matching radius as follows

$$2M < a_0 < \{\frac{M}{12H\pi\zeta_0} - 3K - 3K * ProductLog[-\frac{e^{\frac{M}{36HK\pi\zeta_0}(72HK\pi\zeta_0+24H\pi\zeta_0 r_0^3-r_0)-\frac{r_0^3}{3K}-1}}{72HK\pi\zeta_0}]\}^{\frac{1}{3}}, \tag{60}$$

where $ProductLog$ denotes a set of functions, namely the branches of the inverse function of the function $f(x) = xe^x$.

By fixing the parameters $K = 2$, $H = 73.24$ and $\zeta_0 = 10^{-6}$, we consider the following cases: $r_0/M = 0.25$, in order that $2 < a_0/M < 2.35$; for $r_0/M = 0.1$, we obtain $2 < a_0/M < 2.71$. One can easily find that the range of the junction

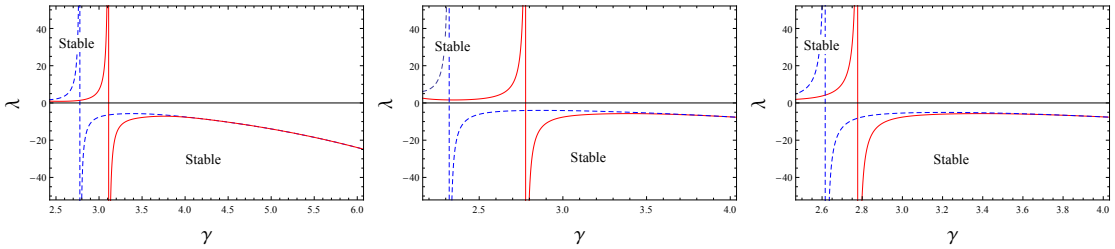

FIG. 3: Plots for a negative surface energy density, i.e., $b(a_0) > 2M$. In the left panel, we set the parameters $K = 2$, $H = 73.24$ and $\zeta_0 = 10^{-6}$ for both cases. The red (solid) and blue (dashed) lines represent $r_0/M = 0.03$ and $r_0/M = 0.01$, respectively. In the medium panel, we set the parameters $K = 2$, $H = 73.24$ and $r_0/M = 0.01$ for both cases. The red (solid) and blue (dashed) lines represent $\zeta_0 = 10^{-6}$ and $\zeta_0 = 10^{-5}$, respectively. In the right panel, we set the parameters $K = 2$, $r_0/M = 0.01$ and $\zeta_0 = 10^{-6}$ for both cases. The red (solid) and blue (dashed) lines represent $H = 73.24$ and $H = 150$, respectively. In the upper half panel, the stability regions are shown above the curves. In the lower half panel, the stability regions are shown beneath the curves.

radius shall decrease for increasing values of r_0/M. Subsequently, we also exhibit the the respective stability regions in the left panel of Fig. 2, and find that, for increasing values of r_0/M, regardless of the decreasing range a_0, the values of the parameter λ are further restricted. Subsequently, we are very interested in investigating the viscous effects on stability of the wormhole configuration. By fixing the parameters $K = 2$, $H = 73.24$ and $r_0/M = 0.1$, we take into account the following cases: $\zeta_0 = 10^{-6}$, so that $2 < a_0/M < 2.71$; for $\zeta_0 = 10^{-10}$, we obtain $2 < a_0/M < 2.619$. It is easy to be seen that the range of the junction radius shall increase for increasing values of ζ_0. In the meanwhile, for decreasing values of ζ_0, regardless of the decreasing range a_0, the values of the parameter λ are further restricted (see the medium panel of Fig. 2). In addition, we also explore about the effects of cosmic background evolution on stability of the wormhole configuration. By fixing the parameters $K = 2$, $r_0/M = 0.1$ and $\zeta_0 = 10^{-6}$, we consider the following cases: $H = 73.24$, in order that $2 < a_0/M < 2.71$; for $H = 150$, we obtain $2 < a_0/M < 2.87$. It is obvious that the range of the junction radius increases for increasing values of H. From the right panel of Fig. 2, we can find that, for decreasing values of H, regardless of the increasing range a_0, the values of the parameter λ are further restricted.

For the case of $b(a_0) > 2M$, we obtain the range of the matching radius as

$$a_0 > \{\frac{M}{12H\pi\zeta_0} - 3K - 3K * ProductLog[-\frac{e^{\frac{M}{36HK\pi\zeta_0}(72HK\pi\zeta_0+24H\pi\zeta_0 r_0^3-r_0)-\frac{r_0^3}{3K}-1}}{72HK\pi\zeta_0}]\}^{\frac{1}{3}}. \tag{61}$$

For $r_0 < 2M$, using the same method described in [42], we just consider the case of $K = 2$. By fixing the parameters $H = 73.24$ and $\zeta_0 = 10^{-6}$, we take into account the following cases: $r_0/M = 0.01$, so that $a_0/M > 2.51$; for $r_0/M = 0.03$, we obtain $a_0/M > 2.45$. The asymptotes $\sigma'|_R = 0$ for these cases situate at $R/M \approx 2.77$ and $R/M \approx 3.12$, respectively. The corresponding stability regions are exhibited in the left panel of Fig. 3. For increasing values of r_0/M, the range of the junction radius increases, the values of the parameter λ are less restricted and one may conclude that the total stability region increase. In the medium panel of Fig. 3, we investigate the viscous effects on stability of the wormhole configuration. Subsequently, we find that, for decreasing values of ζ_0, the range of the junction radius increases, the values of the parameter λ are less restricted and one may still conclude that the total stability region increase. Furthermore, it is very constructive to study the the effects of cosmic background evolution on stability of the wormhole configuration. From the right panel of Fig. 3, we find that, for increasing values of H, the range of the junction radius decreases, the values of the parameter λ are less restricted and one may conclude that the total stability region increase.

For $r_0 > 2M$, we also demonstrate that the values of λ are always negative. By increasing r_0/M, decreasing ζ_0 and increasing H, the values of the parameter λ are less restricted, one may conclude that the total stability region increases, and the range of the junction radius increases, increases and decreases, respectively.

VII. DISCUSSIONS AND CONCLUSIONS

Since the elegant discovery that our universe is undergoing the phase of accelerated expansion, more recently, theorists have gradually paid more and more attention to the exotic spacetime configurations, especially, the renewed field—wormholes. In the literature, all the authors almost construct wormholes by only using the linear equation of state, namely, assuming that the universe is filled with a perfect fluid. Nonetheless, the dynamical behaviors of

the true universe should be physically dominated by a non-ideal cosmic fluid. Therefore, we are very interested in exploring wormholes in the bulk viscosity cosmology.

In this paper, at first, we make a review about the mathematical descriptions of the wormholes. Subsequently, three classes of viscous models are studied, i.e., bulk viscosity as a function of Hubble parameter H, temperature T and dark energy density ρ, respectively. In general, the larger the cosmic expansion velocity H, the smaller the bulk viscosity of the universe is; the larger the cosmic temperature is, the smaller the bulk viscosity of the universe is; the larger the dark energy density, the larger the the bulk viscosity of the universe is. For every model, we solve the Einstein equations by both inserting the shape function $b(r) = r_0 + \frac{1}{K}(r - r_0)$ and the redshift function $\Phi = C$. Since Eq. (18), Eq. (30), Eq. (41) and Eq. (51) can be transformed to each other mathematically by choosing appropriately the parameters ζ_0, ζ_1, H, η, δ, ξ, ϵ, T, γ, β and ρ. Thus, to some extent, these three viscous models have very high degeneracy with each other. In what follows, without the loss of generality, to perform the traversabilities, energy conditions and stability for the wormhole solution, we consider the case of of $\Phi = C$ and $p = -K\rho - 3\zeta_0 H$, namely, the viscous ωCDM with a constant bulk viscosity coefficient. We find that the value of traversal velocity decreases for decreasing bulk viscosity, and the traversal velocity for a traveler depends on not only the wormhole geometry (r_0) but also the effects of cosmological background evolution (K, ζ_0 and H). Subsequently, we find that the NEC will be violated more clearly when the bulk viscosity decreases; the more clearly the NEC is violated, the smaller the cosmic expansion velocity is; the NEC, DEC and SEC are always violated when $r > r_0$, except for $\rho \geqslant 0$ of the WEC is satisfied all the time. Physically, the non-violation of the WEC indicates that the dark energy fluid in the viscous ωCDM model has a non-diverging effect on congruences of null geodesics. However, since the NEC in this case is violated, all the point-wise energy conditions are always violated when $r > r_0$ (see Fig. 1). By implementing the stability analysis, we find that for the case of a positive surface energy density, the range of the junction radius decreases and the values of the parameter λ are further restricted when r_0/M increases, ζ_0 decreases and H decreases, respectively (see Fig. 2); for the case of a negative surface energy density, by increasing r_0/M, decreasing ζ_0 and increasing H, the values of the parameter λ are less restricted, one may conclude that the total stability region increases, and the range of the junction radius increases, increases and decreases, respectively (see Fig. 3).

Note that the condition $0 < \lambda \leqslant 1$ in paper [42], which corresponds to the requirement that the speed of sound should not exceed the speed of light, should be relaxed in the presence of the exotic matter since we still know little about the nature and cosmological origin of the dark energy.

In the future, we expect that more and more highly accurate data can provide newer knowledge about various kinds of celestial bodies and cosmological background evolution for us.

VIII. ACKNOWLEDGEMENTS

We warmly thank Professors Sergei. D. Odintsov and Bharat Ratra for beneficial feedbacks on astrophysics and cosmology. The author Deng Wang thanks Prof. Jing-Ling Chen for helpful discussions about quantum entanglement. The authors acknowledge partial support from the National Science Foundation of China.

[1] A. G. Riess et al., Astron. J. **116**, 1009 (1998).
[2] S. Perlmutter, M. S. Turner, and M. White, Phys. Rev. Lett. **83**, 670 (1999).
[3] Planck Collaboration, [arXiv:1605.02985].
[4] S. Weinberg, Rev. Mod. Phy. **61**, 1 (1989).
[5] E. Witten, [arXiv: hep-th/0106109].
[6] A. Einstein and N. Rosen, Phys. Rev. **48**: 73-77 (1935).
[7] J. A. Wheeler, Phys. Rev. **97**: 511-536, (1955); Geometrodaynamics (Academic, New York, 1962).
[8] M. S. Moris and K.S. Thorne, Am. J. Phys. **56,** 395 (1988).
[9] M. Visser, Phys. Rev. D **39**, 3182 (1989).
[10] E. Poisson and M. Visser, Phys. Rev. D **52**, 7318 (1995).
[11] M. Visser et al., Phys. Rev. Lett. **90**, 201102 (2003).
[12] Oliver James et al., [arXiv:1502.03809v3].
[13] P. F. González-Díaz, Phys. Rev. D **65**, 104035 (2002).
[14] Deng Wang, Xinhe Meng, Eur. Phys. J. C **76**, 171 (2016).
[15] Deng Wang, Xinhe Meng, [arXiv: 1512.03097].
[16] Hristu Culetu, [arXiv:1502.01589].
[17] Mubasher Jamil, Nuovo Cim.B **123**, 599-603, (2008).
[18] C. W. Misner, Astrophys. J. **151**, 431 (1968).
[19] Ø. Grøn, Astrophys. Space Sci. 173, 191 (1990)

[20] Xu Dou, Xinhe Meng, Adv. Astron. **1155**, 829340 (2011).
[21] Zhiyuan Ma, Xinhe Meng, Phys. Lett. B **635**, 186C194 (2006).
[22] S. Nojiri et al., Phys. Rev. D **71**, 063004 (2005).
[23] I. Brevik et al., Phys. Rev. D **70**, 043520 (2004).
[24] L. D. Landau, and E. M. Lifshitz, Fluid Mechanics (Pergamon Press, Oxford 1959).
[25] Xin-He Meng, J.Ren and M.G.Hu, Commun. Theor. Phys. **47,** 379 (2007).
[26] J. Ren and Xin-He Meng, Phys. Lett. B **636,** 5 (2006).
[27] J. Ren and Xin-He Meng, Phys. Lett. B **633,** 1 (2006).
[28] M. G. Hu and Xin-He Meng, Phys. Lett. B **635,** 186 (2006).
[29] Xin-He Meng, X. Dou, Commun. Theor. Phys. **52,** 377 (2009).
[30] S. Nojiri and S. D. Odintsov, Phys. Rev. D **72**, 023003 (2005)
[31] Chaojun Feng and Xinzhou Li, Phys. Lett. B **680**, 355-358 (2009).
[32] F. Rahaman, P. K. F. Kuhfittig, S. Ray, N. Islam, Eur. Phys. J. C **74,** 2750 (2014).
[33] P. K. F. Kuhfittig, Eur. Phys. J. C **462,** 2818 (2014).
[34] F. Rahaman et al., Annals of Physics **350,** 561-567 (2014).
[35] J. F. Navarro, C. S. Frenk, S. D. M. White, Astrophys. J. **462,** 563 (1996).
[36] J. Einasto, Trudy Inst. Astrofiz. Alma-Ata **5,** 87 (1965).
[37] J. Einasto, U. Haud, Galaxy Astron. Astrophys. **223,** 89 (1989).
[38] D. Merritt, A. Graham et al., Astron. J **132,** 6, 2685 (2006).
[39] O.B. Zaslavskii, Phys. Rev. D **72,** 061303(R) (2005).
[40] Deng Wang, Xinhe Meng, [arXiv: 1602.00558].
[41] Deng Wang, Xinhe Meng, [arXiv: 1602.04699].
[42] F. S. N. Lobo, Phys. Rev. D **71**, 124022 (2005).
[43] A. G. Riess et al., Astrophys. J. **826**, 1 (2016).